Calcif Tissue Int (1995) 56:19–25

Calcified
Tissue
International

Factors Influencing Short-Term Precision of Dual X-Ray Bone Absorptiometry (DXA) of Spine and Femur

K. Engelke, C. C. Glüer, H. K. Genant

Department of Radiology, University of California at San Francisco, Osteoporosis Research Group, Box 0628, San Francisco, California 94143, USA

Received: 16 March 1994 / Accepted: 22 July 1994

Abstract. In this study we analyzed the effect of variations in bone area size, baseline soft tissue composition represented by the R-value, and bone region of interest positioning on the precision *in vivo* of bone mineral density (BMD) and content (BMC) as measured by dual X-ray absorptiometry (DXA). The posterior-anterior (PA) spine, decubitus lateral, and femur modes were evaluated. Eleven (PA-spine), 9 (dec-lat), and 14 (femur) postmenopausal women were scanned twice on a Norland XR-26 with repositioning to determine short-term precision of BMD, BMC, AREA, and the R-value. Phantom precisions (CV[%] of 10 consecutive scans) for BMD (BMC) were PA spine: 0.66% (0.57%), neck: 1.1% (1.2%), and trochanter: 0.55% (1.0%). Precisions *in vivo* (CV[%]; two consecutive scans averaged over all patients) were PA spine: 0.9% (1.0%), dec-lat: 7.1% (18%), neck: 1.3% (1.9%), and trochanter: 2.5% (4.9%). BMD precision could be fully explained by BMC and AREA variations. However, BMC alone was a particularly poor predictor of BMD in the dec-lat (r^2 = 0.05) and in the neck (r^2 = 0.13) modes. AREA was a strong predictor for BMC precision explaining between 41% and 88% of the BMC changes. Changes in soft tissue composition contributed significantly in explaining the BMC changes in the dec-lat projection. A higher dependence of BMC changes on AREA changes resulted in a larger difference between BMC and BMD precision. Thus, particularly in the femur and in the decubitus lateral modes, the use of BMD is advantageous compared with BMC.

Key words: DXA — In vivo — Precision — Soft tissue.

Dual X-ray absorptiometry (DXA) has become one of the standard methods in bone densitometry mainly because of its relative ease of use, high precision, the possibility of investigating several different sites within the human body, low radiation dose, and low cost per scan. Newer developments with this technique offer improved lateral measurements of the spine by scanning the patient in the supine instead of the decubitus position. Furthermore, enhancements of the X-ray source intensity and the replacement of pencil beam scanning by fan beam scanning using multiple detectors allow for shorter scan times and the use of solid state detectors like CCDs (charge coupled devices) promises better image quality.

Despite all the technical refinements, the underlying physics of DXA has not changed. For an areal bone mineral density (BMD) determination, the X-ray absorption of two different energies must be measured at two different locations each. One location contains the region of interest (ROI) where the BMD is to be determined, here bone and soft tissue are present. The other location contains just soft tissue that is mostly water-like and fat-equivalent tissue, and is usually referred to as the baseline measurement. In calculating the BMD, one assumes that the X-ray absorption of the soft tissue at both regions is identical. This means in particular that the ratio of lean to fatty tissue is constant. Thus, usually the soft tissue region is in close proximity to the bone region.

Factors influencing DXA precision include quantum noise, patient movement during the investigation, changes in soft tissue composition, patient repositioning between scans, and scan analysis. An increase in dose or the analysis of larger ROIs, e.g., L1–L4 instead of L2–L3 improves the photon counting statistics and reduces quantum noise. Faster scanning reduces the effects of patient movement. Consequently, an increase in dose and faster scans has led to improved precision [1, 2]. However, the radiation dose should be kept as low as possible and an increase in scan speed is limited by the output power of the X-ray source. More powerful X-ray sources tend to be less stable, thus offsetting the gain in precision by faster scanning. Careful repositioning is particularly necessary in scanning the femur and has been subject to several publications [3, 4]. Patient movement and repositioning result in slight differences of the shape and size of the bone ROIs analyzed from scan to scan. This effect is minimized in consecutive phantom scans without repositioning.

This article focuses on three factors potentially influencing BMD and BMC short-term precision in the PA spine, femur, and the decubitus lateral scan modes: (1) changes in the soft tissue composition, (2) changes in the measured bone area size (denoted as AREA throughout the paper), and (3) the influence of bone ROI repositioning (spine in the PA and the decubitus lateral projections only). We will determine whether part of the discrepancy between DXA short-term precision *in vivo* and *in vitro*, which amounts to 0.5–1% in the PA and even higher values in the other scan modes, can be attributed to these factors. As supine lateral measurements were not considered in this article, the terms decubitus lateral and lateral will be used synonymously.

Materials and Methods

DXA Analysis Using Base Materials

This study was carried out using a Norland XR-26 DXA densitom-

Correspondence to: K. Engelke

eter (scan version 1.3.0, analysis version 2.3.Oh). The Norland analysis algorithms use the so-called base material decomposition technique developed by Lehmann and Alvarez [5, 6] who showed that within the X-ray energy range typically applied in medical imaging the absorption of human body materials can be simulated by the absorption of a set of any two so-called basis materials. A change from one set of basis materials to another one is called a *basis material transformation*.

In Norland's case, 'equivalent area densities' of the two base materials, aluminum and polymethylmethacrylate (which will be referred to as acrylic), are calculated for every location along the scan path with the help of a calibration standard. 'Equivalent area densities' means that the X-ray absorption of the acrylic-aluminum combination with these area densities is exactly equal at each energy to the patient absorption at that particular location. Equivalent area densities vary with the applied energy spectrum. The actual BMC is derived by a base material transformation from aluminum and acrylic to calcium hydroxyapatite and soft tissue. Let σ denote equivalent area densities and the indices *b* bone, *st* soft tissue, *a* aluminum, and *p* acrylic. The base material transformation is then described by the following set of linear equations:

$$\sigma_a = c_1\sigma_b + c_2\sigma_{st}$$
$$\sigma_p = c_3\sigma_b + c_4\sigma_{st} \qquad \text{eq. 1}$$

where σ_a and σ_p are measured with the help of the calibration standard for each location along the scan path and c_1–c_4 are constants. c_1 and c_3 can be determined by calibrating σ_a and σ_p against bone mineral or hydroxyapatite. The ratio $R = c_2/c_4$ can be directly measured in the individual subject at a location where no bone is present ($\sigma_b = 0$) which is the so-called baseline soft tissue composition measurement. Thus $R = (\sigma_a / \sigma_p)_{baseline}$. The solution of eq. 1 is straightforward and results in the areal BMD used in DXA:

$$BMD = \sigma_b = \frac{\sigma_a - R\sigma_p}{c_1 - Rc_3}. \qquad \text{eq. 2}$$

Note that at the baseline location, that is in the soft tissue region adjacent to the bone, only the R-value and thus the ratio of equivalent aluminum and acrylic thicknesses enters eq. 2. Accordingly, this parameter will be used in this study. The R-value describes the soft tissue composition. Changes in R can have several reasons, one being a change in the lean/fat ratio. A higher fat content will decrease the R value. The opposite effect will be observed in the presence of any calcium deposits. R is also influenced by the intestinal contents. The BMD calculation assumes that the R-value and thus the soft tissue composition in the baseline and in the bone ROIs are identical. From eq. 2 it is also obvious that a change in R between subsequent scans changes σ_b. Thus, the precision in BMD and BMC is theoretically influenced by the precision in the baseline soft tissue composition.

Special software supplied by Norland permitted the analysis of the base material images which display the equivalent base material thicknesses, in this case aluminum and acrylic, separately. Thus, baseline soft tissue variations between multiple scans of the same patient or from location to locations within a scan could easily be measured. In several ROIs that are described below the equivalent thicknesses of aluminum and acrylic, σ_a and σ_p were measured and their ratio, $R = \sigma_a / \sigma_p$ determined.

Patients

Three different patient groups (G1–G3) were investigated. All patients were postmenopausal women with low BMD (BMD values at least 2 SD below those of young normals). G1: 11 women (age 48–77, mean 64.6), double PA spine scans; G2: 14 women (age 55–91, mean 68.1), double femur scans; G3: 9 women (age 60–79, mean 72.2), double decubitus lateral scans.

Precision

The short-term machine precision *in vitro* was determined by 10 consecutive scans of (1) the Hologic anthropomorphic spine phantom and (2) the Hologic anthropomorphic hip phantom. The phantoms were not repositioned between scans.

For precision *in vivo*, all patients were measured twice with repositioning between the two scans. BMD, BMC, and AREA were derived for the bone regions described below. The R-value was determined for several soft tissue regions, the location and size of which are also described below. The method for calculating the precision is outline below.

PA Spine Measurements

The operator confirmed or corrected the initial settings of the intervertebral markers (horizontal line separating the vertebrae) suggested by the software, and was guided by a histogram showing the integrated density along each scan line. The bone edges separating soft tissue and bone mineral were automatically found. The common parameters, AREA, BMC, and BMD, were calculated for L1–L4 and separately for L2–L3. To obtain optimum precision between the two subsequent scans, the compare function, which displays both scans side by side allowing for a visual comparison of the intervertebral marker placement, was used. The distance between the markers was kept constant for both scans.

In a second step, the influence of the marker placement on precision was investigated. All vertebral markers of the second scan were shifted up or down one scan line from the optimum position. The operator decided whether to shift them up or down according to the criteria of a 'second best position'. Due to patient movement, repositioning, and noise, the two subsequent images were slightly different and visually the second choice in positioning the intervertebral markers actually is often as good as the first one.

The soft tissue composition was determined for vertebral levels L2 and L3 (Fig. 1). Four ROIs (#1–#4) positioned laterally to the spine were analyzed for each level: #1 and #2 were placed as close to the bone edges as possible and had a constant width of 12 mm for all patients and both vertebral levels. #1 was placed on the right side of the spine and #2 on the left site. The height of these two ROIs was identical to the vertebral bodies. #3 and #4, again placed on the right and left site of the spine, covered the total soft tissue region available in the particular scan. Their heights were identical to #1 and #2 which were included in #3 and #4, respectively. However, the widths of #3 and #4 varied from scan to scan and from vertebral level to level as these widths were limited by the scan area. The nonoverlapping parts of ROIs #1 and #3 and of ROIs #2 and #4 are denoted as #5 and #6, respectively (see Fig. 1).

Decubitus Lateral Measurements

Norland's lateral mode requires the operator to select a global region of interest and then generates polygons surrounding the individual vertebrae within which the bone edges are determined. Usually the polygons have to be corrected by the operator and generally two vertebrae—L2–L3 or L3–L4—are analyzed. Exclusion criteria are fractured vertebrae and overlapping ribs or pelvic bones. In our case, only L3 was used. L4 almost always was overlapped by the iliac crest. Ribs overlapping bone or soft tissue at the L2 level cannot always be identified on the DXA scan, however, quantitative computer tomography (QCT) studies show that ribs overlapped the L2 vertebral body in almost 100% of the cases [7, 8]. As in the PA projection, the impact of the operator polygon placement was analyzed. All lateral scans were independently reanalyzed by a second operator.

Similar to the PA soft tissue analysis, two different ROIs were

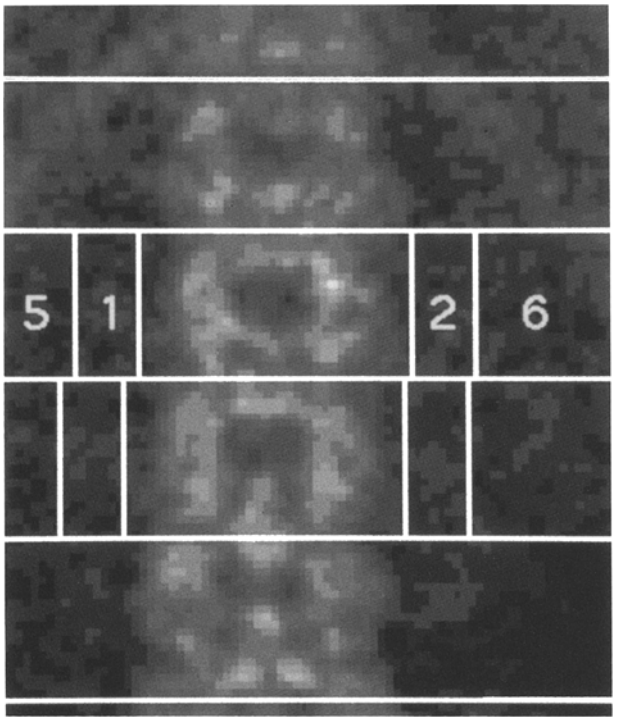

Fig. 1. DXA PA spine image with intervertebral markers. Analyzed soft tissue regions laterally to the spine were analyzed for levels L2 and L3. A total of six regions were analyzed for each level. Regions #3 and #4 are the combined regions #1 + #5 and #2 + #6, respectively.

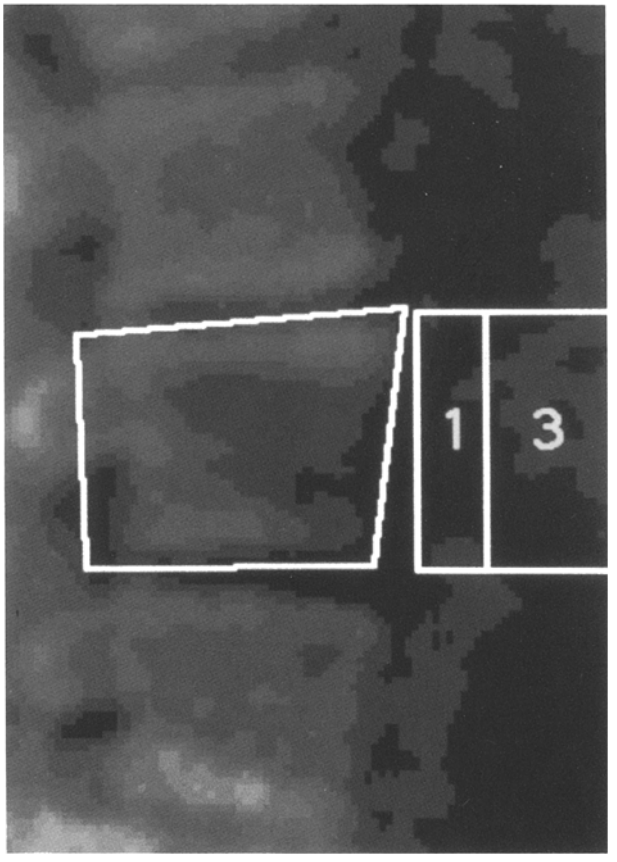

Fig. 2. DXA decubitus lateral spine image. Only the L3 level was used. A total of three regions were analyzed. Region #2 is the combined region #1 + #3.

analyzed (Fig. 2): #1 was placed closely to the bone edges and had a constant bone width of 9 mm for all patients. #2 covered the total soft tissue region available in the scan and included #1. The nonoverlapping area of ROIs #1 and #2 is denoted as ROI #3.

Femur Measurements

BMC, BMD, and AREA of the femoral neck and the trochanteric ROI were analyzed using Norland's standard femur analysis protocol. The analysis is fully automated, however, the operator may interfere and reposition or vary the size of the neck box. The compare feature was used to optimize precision. Soft tissue composition was measured in three different ROIs (Fig. 3): #1 medial of the lesser trochanter, #2 cranial of the greater trochanter extending medially almost to the femoral head, and #3 cranial of the femoral neck; #2 and #3 were partly overlapping. The sizes and locations of these ROIs were kept constant between the two scans but varied a little from patient to patient.

Analysis

The precision results for the phantoms are expressed as coefficients of variation given in % (CV = SD/mean *100). The patient results are expressed as the mean coefficients of variation (CV_M) and their standard deviations (SD). CV_M is calculated by averaging the individual CV values for all patients. SD is not the averaged SD of the individual patients but that of CV_M which reflects the spread of the individual patient CVs around CV_M. CV_M values for BMD, BMC, and AREA were calculated for the two consecutive measurements of each patient. CV_M values for R (R-CV_M) values were calculated for all soft tissue ROIs analyzed.

One-way analysis of variance (ANOVA) was used to analyze inter- and intravertebral level differences of R and R-CV_M in the PA-spine and decubitus lateral scan modes. In the PA mode, intralevel analysis included soft tissue regions #1, #2, #5, and #6 and in the lateral mode #1 and #3. Interlevel differences were analyzed between L2 and L3. In the femur, one-way ANOVA was used to analyze differences of R and R-CV_M among the three soft tissue ROIs.

In order to analyze the impact of bone AREA size changes on BMD and BMC changes, ANOVA of ΔBMD and ΔBMC versus ΔAREA was performed, where Δ denotes the relative difference between the two measurements of the corresponding parameter, e.g., $\Delta BMD = (BMD_{scan2} - BMD_{scan1})/BMD_{average}$. Subsequently, ΔR was included in the models to analyze the impact of the varying soft tissue composition.

Results

BMD/BMC/AREA Precision

The results of the spine and hip phantom measurements are shown in Table 1. An increase of the bone ROI size using the Hologic spine phantom (L1–L4 instead of L2–L3) reduced the BMD-CV from 0.73% to 0.66% and the BMC-CV from 0.63% to 0.57% but increased the AREA-CV from 0.39% to 0.56%. The patient results are shown in Table 2. For the PA spine mode, CV_M is given separately for L1–L4 and L2–L3.

Table 2 also shows the influence of shifting all intervertebral markers one scan line up or down (see Materials and Methods). The results show no significant effect on BMC- and AREA-CV_M. However, the standard variations of the

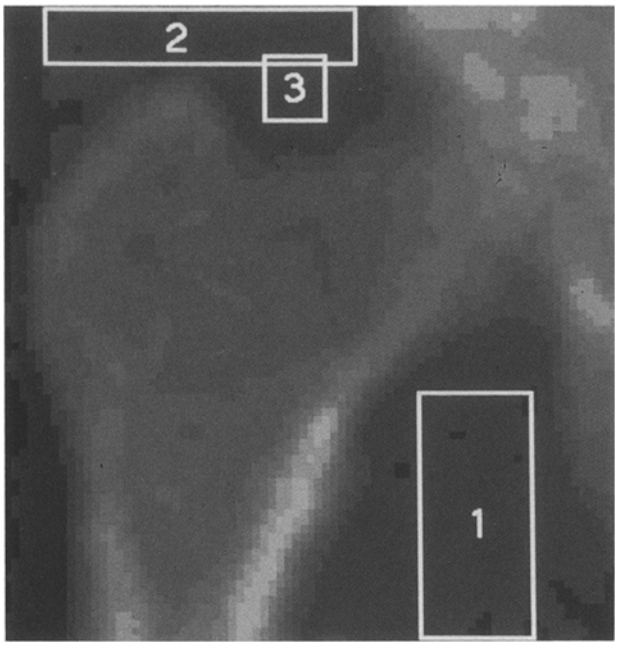

Fig. 3. DXA PA femur image. Three soft tissue regions #1–#3 were used for the analysis.

Table 1. Phantom precision for BMD, BMC, and AREA as %CVs for four different ROIs

Phantoms ROI	CV[%] BMD	BMC	AREA
PA L1–L4	0.66	0.57	0.56
PA L2–L3	0.73	0.63	0.39
Neck	1.1	1.2	0.3
Trochanter	0.55	1.0	1.0

Values result from 10 consecutive scans using the Hologic anthropomorphic spine and hip phantoms

BMC- and AREA-CV_M, that is the spread of the precision data around the mean, is markedly increased. This explains why the differences of the CV_M values for BMC and AREA between shifted and unshifted ROIs are statistically nonsignificant although the CV_M values differ by approximately a factor of 2. The BMD values are even less affected by a slight shift of the intervertebral spaces. There was a moderate increase in the SD of the mean CV from 0.4 to 0.9 but the CV_M value was almost constant (0.9 for the unshifted and 1.0 for the shifted ROI).

In order to verify the rather poor precision results derived in the lateral projection, all scans were carefully reanalyzed by a second operator. This reanalysis changes the bone ROIs slightly as the polygons around the vertebral bodies are redefined. The results of this reanalysis confirmed the data given in Table 2. It should be kept in mind that only one vertebral level was analyzed. Thus, the precision cannot be as good as in the PA mode. Averaging over four vertebrae theoretically improves the precision by a factor of 2 compared with the analysis of one vertebra. But even taking this effect into consideration, the precision measured in the lateral projection is worse by approximately a factor of 3-4 compared with the precision in the PA mode.

Soft Tissue Composition Precision

The soft tissue precision *in vivo* analysis is summarized in Table 3. Compared with the BMD precision, the soft tissue precision is markedly reduced in the PA projection and in the femur but is comparable in the decubitus spine mode. In the PA projection, one-way ANOVA showed neither significant inter- nor intralevel soft tissue variations. The analysis was performed separately for R (intralevel: $F < 0.4$, $P > 0.7$, interlevel: $F < 1.6$, $P > 0.2$), and R-CV_M (intralevel: $F < 0.75$, $P > 0.5$, interlevel: $F < 3.5$, $P > 0.07$). However, the mean R value (averaged over all patients) at vertebral level L3 was approximately 20% lower and the R-CV_M value two to three times higher compared with level L2. Thus, larger patient numbers will potentially result in significant interlevel differences.

As in the PA projection, significant ROI soft tissue composition differences were found neither in the lateral projection nor in the femur scan mode. One-way ANOVA gave the following results: dec-lat R ($F < 0.4$, $P > 0.8$), dec-lat R-CV_M ($F = 0.3$, $P = 0.6$); femur R ($F = 0.4$, $P = 0.7$), and femur R-CV_M ($F = 0.4$, $P = 0.7$).

Impact of AREA and Soft Tissue Composition on BMD and BMC Precision

The results of the ANOVA for ΔBMD and ΔBMC are summarized in Tables 4 and 5. The overall significance of the corresponding models is given as the P-value. Further, standard errors of the estimate (SEE), and the squared regression coefficients r^2 of the analysis and the levels of significance of the independent variables are given.

As expected, BMD variations can be fully explained by BMC and AREA variations. In all scan modes the squared regression coefficients were $r^2 > 0.996$ and the models were highly significant. ΔR was not a significant predictor for BMD in the PA spine and in the femur. In the lateral spine, however, variations of R in soft tissue ROI #1 that is in the ROI directly adjacent to the vertebra variation contributed significantly ($P < 0.001$) to ΔBMD. An inclusion of ΔR in the ANOVA decreased the SEE by a factor of 5 from 0.004 to 0.0008 and increased r^2 from 0.999 to 1.0. Although significant, this effect is very small as more than 99.9% of the total BMD variation is already explained by BMC and AREA variations. Soft tissue variations from ROI #2 and 3 produced no significant effect.

ΔBMC was a poor predictor for ΔBMD in the lateral projection and in the neck region where less than 15% of the BMD variation could be explained by BMC variations alone. This value increased to 34% in the trochanter and to 43% in the PA projection including L1–L4. In the L2–L3 vertebral levels, 79% of the BMD variation could be explained by BMC variations alone.

The ΔBMC analysis gave the following results: Except for the L2–L3 region ΔAREA alone was a strong predictor explaining between 41% and 88% of the BMC changes. An additional inclusion of ΔR as predictor of ΔBMC had no effect in the PA projection. Also in the femur mode, ΔR was a nonsignificant ($P > 0.05$) predictor of ΔBMC. In the lateral mode, an inclusion of ΔR from soft tissue ROI #2 was significant and improved the overall prediction of the model: r^2 increased from 0.88 to 0.95 and the SEE decreased from 0.11 to 0.08. In the neck ROI, an inclusion of ΔR in the model increased r^2 slightly (average value of St-ROIs #1–#3: $r^2 = 0.85$), the SEE did not change, and the significance of the overall models remained high ($P < 0.002$). In the trochanter,

Table 2. Precision *in vivo* for BMD, BMC, and AREA as average CV and their SDs ($\overline{CV}$[%] ± SD[%]) for five different ROIs

In vivo ROI	$\overline{CV}$[%] ± SD[%]			PA-mode: ROI shifted one pixel up or down dec-lat mode: reanalysis by different operator $\overline{CV}$[%] ± SD[%]		
	BMD	BMC	AREA	BMD	BMC	AREA
PA L1–L4	0.9 ± 0.4	1.0 ± 0.8	0.9 ± 0.5	1.0 ± 0.7	1.9 ± 3.3	2.1 ± 3.2
PA L2–L3	1.8 ± 1.0	1.7 ± 1.0	0.8 ± 0.6	1.9 ± 1.2	3.5 ± 6.0	3.1 ± 5.7
dec-lat L3	7.1 ± 3	18 ± 12	17 ± 15	8.4 ± 4	17 ± 13	17 ± 17
Neck	1.3 ± 1.1	1.9 ± 2.2	2.0 ± 1.8			
Trochanter	2.5 ± 2.5	4.9 ± 3.4	4.2 ± 2.6			

The %CV values from two consecutive scans of postmenopausal women with repositioning were averaged over all women in each group (n = 11 for PA spine; n = 6 for dec-lat; n = 14 for PA proximal femur). Also, for the spine, the $\overline{CV}$ values after repositioning are shown

Table 3. Soft tissue precision *in vivo* in the spine and the femur

Projection	$\overline{CV}$[%] ± SD[%]	ROI #
PA L2	2.0 ± 1.2	3 + 4
PA L3	7.0 ± 9.4	3 + 4
dec-lat L3	5.4 ± 6.7	2
Femur	4.5 ± 6.2	1 + 3

The soft tissue regions used for the precision analysis are indicated in the ROI # row. See Figs. 1–3 for an exact location of the soft tissue regions

an effect was only observed for St-ROI #4: ($r^2 = 0.82$, $P = 0.0002$ and SEE = 0.0).

Discussion

The observed BMD precision values in Table 1 are in the range previously reported: around 0.5% for phantom measurements [4, 9–12, 13], 0.8–1.0% (young healthy normals) for L2–L4 PA-projection [11, 14–16], 0.6% (young healthy) to 3.3% (elderly osteoporotic females) in the trochanteric region, 1.0% (young healthy) to 2.1% (postmenopausal females) in the neck region [4, 15, 17–22], and 2.7–5.5% (analysis of two vertebrae) and 6.4% (analysis of a single vertebra) in the decubitus lateral projection [23–26].

Scanning larger areas markedly improved the precision *in vivo*, although little change was measured *in vitro*, indicating that photon noise is not the primary error source *in vivo*. A statistical analysis using a paired *t*-test comparing the mean coefficients of variations, that is, the precision of BMD and BMC, showed no significant differences between BMD- and BMC-CV_M values. However, the SD of the BMD-CV_M is considerably lower than the BMC-CV_M. In addition, BMD shows higher power to predict fractures than BMC. Thus, BMD is a more reliable predictor for BMD differences in cross-sectional studies.

The superiority of BMD over BMC regarding precision was also demonstrated when we investigated the effect of repositioning all intervertebral markers vertically by one pixel in the PA projection. Table 2 shows that the BMC and AREA precision values were decreased while the repositioning did not effect BMD precision. A reanalysis of the lateral scans did not significantly change the already poor precision values. Thus, the analysis software is relatively insensitive to small changes in the separation of the vertebral body from the spinal process. These results show that as long as the analysis is done in agreement with the manufacturers specifications, the BMD precision does not change drastically and that in particular, the low precision in the lateral projection cannot be attributed to operator interactions.

BMD precision could be fully explained by BMC and bone AREA size variations. This is not a surprising result, as BMD is just the ratio of BMC and AREA. Also of interest is the degree of BMD variation which can be explained by BMC variation alone. The results were particularly low for the lateral mode and the neck where less than 15% of the BMD variation could be explained by the BMC variation alone. The overall models for these ROIs were not significant. In the trochanter 34% and in the PA spine (L1–L4) 43% of the BMD variation could be explained and the overall models were borderline significant. It must be pointed out that BMC itself implicitly depends on AREA, thus in the ΔBMD versus ΔBMC regression the AREA influence still exists. It is interesting to see that for those scan sites where the BMC precision error was higher than the BMD precision error like in the femur and in the lateral projections, the regression coefficients between ΔBMD and ΔBMC were poor ($r^2 < 0.4$) but those between ΔBMC and ΔAREA were high ($r^2 > 0.6$). A higher dependence of ΔBMC on bone AREA size changes resulted in a lower dependence of ΔBMD on ΔBMC and a larger difference between BMC and BMD precision. The influence of the AREA variations partly offset the BMC variations, i.e., in using BMD instead of BMC, a major error source cancels out.

The influence of soft tissue composition was previously investigated by Valkema et al. [27] using dual photon absorptiometry. They calculated that the baseline soft tissue variation caused a BMC-CV_M of 0.7% in normals and 1.5% in osteoporotics and measured a total BMC-CV_M of 1.6% in normals and 2.6% in osteoporotics. Because they did not publish phantom precision data of their scanner (Novo BMC-Lab22a) nor did they perform a regression analysis between soft tissue and BMC variations, it remains difficult to assess the influence of soft tissue on BMC variations based on their data.

In our study, some of the BMC variations in the femur and in the lateral mode could be explained by soft tissue composition variations. Our analysis of the impact of soft tissue composition on BMD precision gave nonsignificant or negligible results. These results do not encourage any further efforts to improve the patient individual short-term BMD or BMC precision by using soft tissue information. However, in

Table 4. ANOVA results for ΔBMD (independent variable)

Projection	Independent variables	ANOVA	Independent variables	ANOVA
PA L1–L4	Const$^+$	$P = 0.04$	Const^a	$P < 0.00001$
	ΔBMC^a	$r^2 = 0.43$	ΔBMD^c	$r^2 = 1$
		SEE = 0.01	ΔAREA^c	SEE < 0.0001
PA L2–L3	Const$^+$	$P = 0.0006$	Const$^+$	$P < 0.00001$
	ΔBMC^c	$r^2 = 0.79$	ΔBMC^c	$r^2 = 1$
		SEE = 0.014	ΔAREA^c	SEE < 0.0001
dec-lat	Const$^+$	$P = 0.99$	Const$^+$	$P < 0.00001$
L3	ΔBMC$^+$	$r^2 = 0.01$	ΔBMC^c	$r^2 = 0.999$
		SEE = 0.03	ΔAREA^c	SEE < 0.004
Neck	Const$^+$	$P = 0.22$	Const^a	$P < 0.00001$
	ΔBMC$^+$	$r^2 = 0.13$	ΔBMC^c	$r^2 = 1$
		SEE = 0.023	ΔAREA^c	SEE < 0.0001
Trochanter	Const$^+$	$P = 0.036$	Const^a	$P < 0.00001$
	ΔBMC^a	$r^2 = 0.34$	ΔBMC^c	$r^2 = 0.996$
		SEE = 0.04	ΔAREA^c	SEE < 0.0033

The overall significance of the models are given as the *p*-value. Further, SEE, squared regression coefficients r^2, and levels of significance of the independent variables of the specific model are shown ($^+$ns; $^aP < 0.05$, $^bP < 0.01$, $^cP < 0.001$). ΔR was only a significant contributor in the dec-lat mode (see text).

Table 5. ANOVA results for ΔBMC (independent variable)

Projection	Independent variables	ANOVA
PA L1–L4	Const$^+$	$P = 0.045$
	ΔAREA^a	$r^2 = 0.41$
		SEE = 0.014
PA L2–L3	Const$^+$	$P = 0.47$
	ΔAREA$^+$	$r^2 = 0.07$
		SEE = 0.03
dec-lat	Const$^+$	$P = 0.0002$
Le	ΔAREA^b	$r^2 = 0.88$
		SEE = 0.11
Neck	Const$^+$	$P = 0.0005$
	ΔAREA^c	$r^2 = 0.68$
		SEE = 0.024
Trochanter	Const$^+$	$P = 0.0001$
	ΔAREA^c	$r^2 = 0.76$
		SEE = 0.048

Again, ΔR was only a significant contributor in the dec-lat mode (see text).^{a,b,c} Same as Table 4; $^+$ns

large cross-sectional studies or longitudinal studies there may be some benefits to looking at the soft tissue composition more closely.

In our study, we analyzed only short-term precision, including repositioning of the patients. We did not investigate how the BMD/BMC accuracy or longer-term precision is affected by soft tissue variations and in particular by the fat distribution. Several other publications cover this topic [28–31]. The emphasis of our study was to explain the difference between short-term precision *in vivo* and *in vitro*. Apart from machine instabilities and photon noise, which account for approximately 0.5–1% of the precision error, the main contributor seems to be repositioning of the patient. The reader should keep in mind that our AREA analysis involved only its size, not its location. A change in the projected area caused by repositioning between the two scans or movement during the scan will result in changes of the contours outlining the bone regions. With regard to the BMD precision, a change in AREA size will in part be offset by a corresponding change in BMC. A change in AREA shape without a change of its size will change the BMC but not the AREA value and thus have a greater impact on the BMD value.

Although we used a Norland XR26 scanner in our study, we do not expect that the analysis of similar data in the PA spine and femur projections using a different DXA system will result in major differences compared with the data presented here. The physical principles of all DXA systems currently in use are very similar, although certain hardware and software implementations like the X-ray detector configuration or the bone edge detection may vary among the systems. In the lateral scan mode, however, recently introduced equipment like the Hologic 2000 DXA or the Lunar Expert systems allow supine instead of decubitus positioning. In addition, the Hologic system combines a supine lateral analysis with a PA analysis which greatly improves the short-term precision *in vivo*. Thus, results for the decubitus lateral scan mode presented in this publication may change when supine lateral scan will be analyzed instead.

Conclusion

Short-term precision *in vivo* and *in vitro* values for AP spine, decubitus lateral, and AP femur projections measured in this study are in agreement with earlier studies. Precision values for BMC and BMD values showed no significant differences but the SD was considerably lower for BMD-CV_M, thus BMD is a more reliable predictor for BMD differences in cross-sectional studies. BMD precision in the PA spine and lateral projections precision showed no significant effect after a slight repositioning of the analyzed ROIs in the follow-up scan, although the SD of the averaged CV was increased. BMC and AREA precision were markedly (although statistically nonsignificant) increased after repositioning.

BMD variations can be fully explained by BMC and bone AREA size variations ($r^2 > 0.996$). BMC precision alone is a poor predictor for BMD precision, in particular in the decubitus lateral ($r^2 = 0.05$) and in the femoral neck regions ($r^2 = 0.13$). The relationship between BMC and AREA variations depends on the particular site. ΔAREA was a bad predictor for L2–L3 ($r^2 = 0.07$) and a good predictor for decubitus lateral ($r^2 = 0.92$). The larger the difference between BMD

and BMC variations the higher the predictive power of ΔAREA for ΔBMC. Soft tissue variations had an impact on BMD precision in the lateral mode by reducing the standard error of the estimate of the linear model. Also, soft tissue variations explain some BMC variations in the femur and in the lateral, that is, in those sites where the differences between precision *in vitro* and *in vivo* is high; however, our results do not encourage efforts to improve individual patient short-term BMD or BMC precision *in vivo* by a soft tissue variation analysis. The main effect explaining the difference between precision *in vivo* and *in vitro* is patient repositioning.

Acknowledgments. We greatly appreciate support and suggestions from Russ Nord (Norland Corporation, Fort Atkinson, WI, USA).

References

1. Sorensen JA (1991) Relationship betwwen patient exposure and measurement precision in dual photon absorptiometry of the spine. Phys Med Biol 36:169–176
2. Mazess R, Chesnut CH III, McClung M, Genant HK (1992) Enhanced precision with dual-energy x-ray absorptiometry. Calcif Tissue Int 51:14–17
3. Wilson CR, Fogelman I, Blake GM, Rodin A (1991) The effect of positioning on dual energy x-ray bone densitometry of the proximal femur. Bone Miner 13:69–76
4. Lilley J, Walters BG, Heath DA, Drolc Z (1991) In vivo and in vitro precision of bone density measured by dual-energy x-ray absorption. Osteoporosis Int 1:141–146
5. Lehmann LA, Alvarez RE, Macovski A, Brody WR (1981) Generalized image combinations in dual-kVp-digital radiography. Med Phys 8:659–667
6. Alvarez RE, Macovski A (1976) Energy-selective reconstructions in x-ray computerized tomography. Phys Med Biol 21: 733–744
7. Schmitz S, Steiger P, Melnikoff S, Lang P, Genant HK (1990) Lateral x-ray dual absorptiometry of the spine: estimating soft-tissue inhomogeneity with CT. In: Proceedings of 76th Scientific Assembly and Annual Meeting Radiological Society of North America, Chicago, Radiology, p 172
8. Rupich RC, Griffin MG, Pacifici R, Avioli LV, Susman N (1992) Lateral dual-energy radiography: artifact error from rib and pelvic bone. J Bone Miner Res 7:97–101
9. Lai KC, Goodsitt MM, Murano R, Chesnut CH III (1992) A comparison of two dual-energy x-ray absorptiometry systems for spinal bone mineral measurement. Calcif Tissue Int 50:203–208
10. Kelly TL, Slovik DM, Neer RM (1989) Calibration and standardization of bone mineral densitometers. J Bone Miner Res 4(5):663–669
11. Cullum ID, Ell PJ, Ryder JP (1989) X-ray dual photon absorptiometry: a new method for the measurement of bone density. Br J Radiol 62:587–592
12. Orwoll ES, Oviatt SK (1991) Longitudinal precision of dual-energy x-ray absorptiometry in a multicenter study. J Bone Miner Res 6:191–197
13. Rencken ML, Murano R, Drinkwater L, Chesnut CH (1991) In vitro comparability of dual energy x-ray absorptiometry (DXA) bone densitometers. Calcif Tissue Int 48:245–248
14. Hansen MA, Hassager C, Overgaard K, Merslew U, Riis BJ, Christiansen C (1990) Dual energy x-ray absorptiometry: a precise method of measuring bone mineral density in the lumbar spine. J Nucl Med 0:00–00
15. Pouilles J-M, Tremollieres F, Todorovsky N, Ribot C (1991) Precision and sensitivity of dual-energy x-ray absorptiometry in spinal osteoporosis. J Bone Miner Res 6:997–1002
16. Slosman DO, Rizzoli R, Buchs B, Piana F, Donath A, Bonjour J-P (1990) Comparative study of the performances of x-ray and gadolinium 153 bone densitometers at the level of the spine, femoral neck and femoral shaft. Eur J Nucl Med 17:3–9
17. Duboeuf F, Braillon P, Chapuy MC, Haond P, Hardouin C, Meary MF, Delmas PD, Meunier PJ (1991) Bone mineral density of the hip measured with dual-energy x-ray absorptiometry in normal elderly women and in patients with hip fracture. Osteoporosis Int 242–249
18. Glüer CC, Steiger P, Selvidge R, Elliesen-Kliefoth K, Hayashi C, Genant HK (1990) Comparative assessment of dual-photon-absorptiometry and dual-energy-radiography. Radiology 174: 223–228
19. Lees B, Stevenson JC (1992) An evaluation of dual energy x-ray absorptiometry and comparison with dual-photon absorptiometry. Osteoporosis Int 2:146–152
20. Johnson J, Dawson-Hughes B (1991) Precision and stability of dual energy x-ray absorptiometry measurements. Calcif Tissue Int 49:174–178
21. Haddaway MJ, Davie MWJ, McCall IW (1992) Bone mineral density in healthy normal women and reproducibility of measurements in spine and hip using dual-energy x-ray absorptiometry. Br J Radiol 65:213–217
22. Sievänen H, Oja P, Vuori I (1992) Precision of dual-energy x-ray absorptiometry in determining bone mineral density and content of various skeletal sites. J Nucl Med 33:1137–1142
23. Larnach TA, Boyd SJ, Smart RC, Butler SP, Rohl PG, Diamond TH (1992) Reproducibility of lateral spine scans using dual energy x-ray absorptiometry. Calcif Tissue Int 51:255–258
24. Reid IR, Evans MC, Stapleton J (1992) Lateral spine densitometry is a more sensitive indicator of glucocorticoid-induced bone loss. J Bone Miner Res 7:1221–1225
25. Slosman DO, Rissoli R, Donath A, Bonjour J-P (1990) Vertebral bone mineral density measured laterally by dual-energy x-ray absorptiometry. Osteoporosis Int 1:23–29
26. Souza A, Nakamura T, Shiraki M, Stergiopoulos K, Ouchi Y, Orimo H (1990) Measurement of vertebral body using dual energy x-ray absorptiometry in lateral projection. In: Christiansen C, Overgaard K (eds) Proceedings of Osteoporosis. Copenhagen, Denmark, Osteopress ApS, pp 640–642
27. Valkema R, Verheij LF, Blockland JAK, Zwindermann AH, Bijvoet OLM, Papapoulos SE, Pauwels EKJ (1990) Limited precision of lumbar spine dual photon absorptiometry by variations in the soft-tissue background. J Nucl Med 31:1774–1781
28. Hangartner TN, Johnston CC (1990) Influence of fat on bone measurements with dual-energy absorptiometry. Bone Miner 9:71–81
29. Sorenson JA (1990) Effects on nonmineral tissues on measurement of bone mineral content by dual-photon absorptiometry. Med Phys 17:905–912
30. Farrell TJ, Webber CE (1989) The error due to fat inhomogeneity in lumbar spine bone mineral measurements. Clin Phys Physiol Meas 10:57–64
31. Tothill P, Pye DW (1991) Errors in DXA of spine due to non-uniform fat distribution. Osteoporosis Int 1:199